IJST, Transactions of Mechanical Engineering, Vol. 35, No. M1, pp 73-83
Printed in The Islamic Republic of Iran, 2011

MIXED CONVECTION SIMULATION OF INCLINED LID DRIVEN CAVITY USING LATTICE BOLTZMANN METHOD*

A. A. RABIENATAJ DARZI, M. FARHADI,** K. SEDIGHI, E. FATTAHI AND H. NEMATI
Dept. Mechanical Engineering, Babol University of Technology, Babol, I. R. of Iran, P.O. Box: 484
Email: mfarhadi@nit.ac.ir

Abstract– In this study, the mixed convective heat transfer in a lid driven square cavity at different inclination angles is investigated numerically using lattice Boltzmann method with Boussinesq approximation. The vertical walls of the cavity are insulated, while the bottom (hot wall) and top (cold lid) surface are maintained at a uniform temperature. The study is carried out for Richardson numbers ranging from 0.01 to 10 and an inclination angle of cavity ranging from 90 to 90. These Richardson numbers are selected based on the inclusion of forced, mixed and natural effects. The result shows that the heat transfer rate is independent of the inclination angle for Ri of 0.01, whereas it changes when the Richardson number increases. Moreover, it has been found that this effect is positive for negative angles and negative for positive angles that are due to the effect of buoyancy force on flow field. In addition, the verity of Nusselt number and Richardson number are opposite because the natural convection changes to mixed or forced convection when the Richardson number decreases. Consequently the Nusselt number increases.

Keywords– Lattice Boltzmann method, mixed convection, lid-driven cavity, Richardson number

1. INTRODUCTION

In recent years the natural and mixed convection in a cavity has been investigated by many researchers [1-5]. This attempt is due to the fact that heat transfer in a square cavity can be found in many industrial and engineering applications such as electronic component cooling, food drying process, nuclear reactors etc. Moallemi and Jang [6] studied the effect of Prandtl number and Reynolds number on the flow and thermal characteristics of a laminar mixed convection in a rectangular cavity. Prasad and Koseff [7] reported experimental results on mixed convection heat transfer process in a lid-driven cavity for a different Richardson number ranging from 0.1 to 1000. Heat transfer results for mixed convection from a bottom heated open cavity subjected to an external flow studied for a wide range of the governing parameters (i.e., $1 \le Re \le 2000$, $0 \le Gr \le 10^6$) over cavities with various aspect ratios (A = 0.5, 1, 2 and 4) were reported by Leong et al.[8]. A numerical study was presented by Singh and Sharif [9] to investigate mixed-convective cooling of a two-dimensional rectangular cavity with differentially heated vertical sidewalls. Influence of the Reynolds number, Richardson number, and location of inlet and outlet openings on the flow field and thermal field have been discussed. Their result indicated that maximum cooling efficiency, minimum average temperature, and maximum Nusselt number at the hot surface occurs when the inlet is situated at the bottom of the cold wall and the outlet is situated at the top of the hot wall. Basak et al. [10] investigated the influence of uniform and non-uniform heating of bottom wall on mixed convection lid driven flows in a square cavity. A complete study on the effect of Grashof number (Gr) shows that the strength of circulation increases when increasing the value of the Gr number irrespective of Re and Pr

*Received by the editors May 5, 2010; Accepted December 6, 2010.
**Corresponding author

number. As the value of the Gr number increases, a transition occurs from conduction to convection dominated flow at Gr=5×10^3 and Re=1 for Pr=0.7.

The lattice Boltzmann (LB) method is a powerful approach to hydrodynamics, with applications ranging from large Reynolds number flows to flows at a micron scale, modeling the physics in fluids [11-14]. Various numerical simulations have been performed using different thermal LB models or Boltzmann-based schemes to investigate the natural convection problems [15-22].

Kao et al. [23] investigates 2D natural convection flows with nonlinear phenomena within enclosed rectangular cavities using simple lattice Boltzmann (LB) thermal model with the Boussinesq approximation. They found that unstable flow is generated at particular values of the Rayleigh number, Knudsen number, and cavity aspect ratio.

In the present study, the effect of inclination angle on heat transfer rate and flow pattern inside of lid-driven square cavity is investigated numerically by lattice Boltzmann methods at different Richardson numbers.

2. COMPUTATIONAL METHODOLOGY

The LB model used here is the same as that employed in [19-21]. The thermal LB model utilizes two distribution functions, f and g, for the flow and the temperature field, respectively. It uses modeling of movement of particles to capture macroscopic fluid quantities such as velocity, pressure and temperature. In this approach the fluid domain is discretized in uniform Cartesian cells. Each cell holds a fixed number of distribution functions, representing the number of particles moving in these discrete directions. For this work, the most popular model for the 2D case, the D2Q9 model, which consists of 9 distribution functions, has been used. The values of $w_0 = 4/9$ for $|c_0| = 0$ (for the static particle), $w_{1-4} = 1/9$ for $|c_{1-4}| = 1$ and $w_{5-9} = 1/36$ for $|c_{5-9}| = \sqrt{2}$ are assigned for this model.

The density and distribution functions i.e. the f and g, are calculated by solving the Lattice Boltzmann equation (LBE), which is a special discretization of the kinetic Boltzmann equation. After introducing BGK approximation, the general form of lattice Boltzmann equation with external force can be written as:

$$f_i(x + c_i\Delta t, t + \Delta t) = f_i(x,t) + \frac{\Delta t}{\tau_\upsilon}[f_i^{eq}(x,t) + f_i\ (x,t)] + \Delta t.c_i.F_i \tag{1}$$

for the flow field and

$$g_i(x + c_i\Delta t, t + \Delta t) = g_i(x,t) + \frac{\Delta t}{\tau_D}[g_i^{eq}(x,t) + g_i(x,t)] \tag{2}$$

for the temperature field

Where Δt denotes lattice time step, c_k is the discrete lattice velocity in direction *k*, F_i is the external force in direction of lattice velocity, and τ_υ and τ_D denote the lattice relaxation time for the flow and temperature field. The kinetic viscosity υ and the thermal diffusivity α, are defined in terms of their respective relaxation times, i.e. $\upsilon = c_s^2(\tau_\upsilon - 1/2)$ and $\alpha = c_s^2(\tau_D - 1/2)$, respectively. Note that the limitation 0.5 < τ should be satisfied for both relaxation times to ensure that viscosity and thermal diffusivity are positive. Furthermore, the local equilibrium distribution functions are calculated with Eq. (3, 4) for the flow and the temperature field, respectively.

$$f_i^{eq} = w_i\rho[1 + \frac{c_i.u}{c_s^2} + \frac{1}{2}\frac{(c_i.u)^2}{c_s^4} - \frac{1}{2}\frac{u^2}{c_s^2}] \tag{3}$$

$$g_i^{eq} = w_i.T(x,t)[1+\frac{c_i.u}{c_s^2}] \tag{4}$$

Where w_k is a weighting factor, ρ is the lattice fluid density.

In order to incorporate buoyancy force in the model, the force term in the Eq. (1) needs to be calculated as follows:

$$F_i = 3w_i\beta\theta\,\vec{g} \tag{5}$$

The Boussinesq approximation is applied and radiation heat transfer is negligible.

To ensure that the code works in near incompressible regime, the characteristic velocity of the flow $|\vec{u}| = \sqrt{\beta\,\vec{g}\Delta TH}$ must be small compared with the fluid speed of sound. In the present study, Mach number was taken to be equal to 0.1.

Finally, macroscopic variable can be calculated in terms of these variables, with the following formula.

Flow density: $$\rho = \sum_k f_k \tag{6}$$

Momentum: $$\rho u_i = \sum_k f_k c_{ki} \tag{7}$$

Temperature: $$T = \sum_k g_k \tag{8}$$

The kinetic viscosity and thermal diffusivity are calculated from the characteristic velocity through the following relationships, respectively:

$$\upsilon^2 = \frac{u^2H^2\,\mathrm{Pr}}{Ra}, \alpha = \frac{\upsilon}{\mathrm{Pr}} \tag{9}$$

The relaxation times, τ_υ and τ_D, for flow and temperature LB equations given in Eqs. (1) and (2) can then be determined. This implies that kinetic viscosity (υ) and thermal diffusivity (α) cannot be considered as constants in LBM simulations if the characteristic velocity (u) is kept constant. For determining an appropriate characteristic velocity, we used a model based on the principle of kinetic theory.

The Knudsen number for this geometry can be written as (Kao et al. [23]):

$$Kn \equiv \frac{\lambda}{H} = \sqrt{\frac{\pi\gamma}{2}}\frac{\upsilon}{c_s H} \tag{10}$$

Where Ma is the Mach number, Re is the Reynolds number, and the heat capacity ratio is to be γ = 5/3 for a monatomic ideal gas and γ = 7/5 for a diatomic gas according to the definition of mean free path, $\lambda = \sqrt{\frac{\pi\gamma}{2}}\frac{\upsilon}{c_s}$.

From the definition of Rayleigh number and Eq (10):

$$u^2 = \frac{Ra.Kn^2.c_2^2}{\pi\gamma\,\mathrm{Pr}/2}, \qquad \text{where } c_s^2 = \frac{c^2}{3} \tag{11}$$

Details of this model are available in [23]**.** By this definition, the characteristic velocity is a function of the Rayleigh number, Knudsen number, Prandtl number and the value of c, all of which are specified as given values in LBM simulations which include the macroscopic and mesoscopic scales at natural convection problems.

3. COMPUTATIONAL DOMAIN AND VALIDATION

The treated problem is a two dimensional square lid-driven cavity in different cases with a side length H. The computational domain considered in the present study is shown in Fig. 1. The vertical walls are assumed adiabatic, while the horizontal walls are maintained at a uniform temperature. The top and bottom walls are considered as cold and hot walls, respectively. The top wall moves at a constant speed. During this study the Grashof number was fixed at 10^4 so that the Richardson number changes with Reynolds number. In addition, the Prandtl number is 1.0.

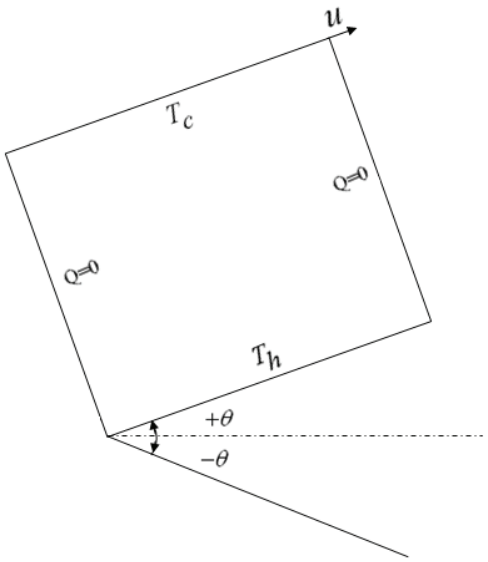

Fig. 1. Schematic of computational domain

The Grashof number (Gr) and Nusselt number (Nu) for the current problem are defined as follows:

$$Gr = g\,\beta\Delta T H^3 / \upsilon^2 \tag{12}$$

$$Nu_L = -(\frac{\partial T}{\partial y}) \tag{13}$$

The averaged Nusselt number is calculated by integrating the local Nusselt number along the surface of the step as:

$$Nu_{av} = \frac{1}{L}\int_0^L Nu_y dx \tag{14}$$

A comparison was conducted while employing the following dimensionless parameters: Re = 500, Ri = 0.4 and Pr = 1. Validation was performed by comparing the streamlines and the local Nusselt number distribution along the cavity lid between the present work and Moallemi and Jang [6]. Comparison shows excellent agreement for both streamlines and local Nusselt distributions as displayed in Figs. 2 and 3.

The averaged Nusselt number over the bottom wall (hot wall) is a good indicator of grid independence. The study of grid dependency has been performed at Ri=0.4 and for three non-uniform grids. Results show that, when the number of grid points pass from a 50× 50 to 80× 80 and after to 120× 120, the averaged Nusselt number increases 5.37% and 0.6% respectively. Therefore, the grid of 80× 80 is sufficient for this simulation.

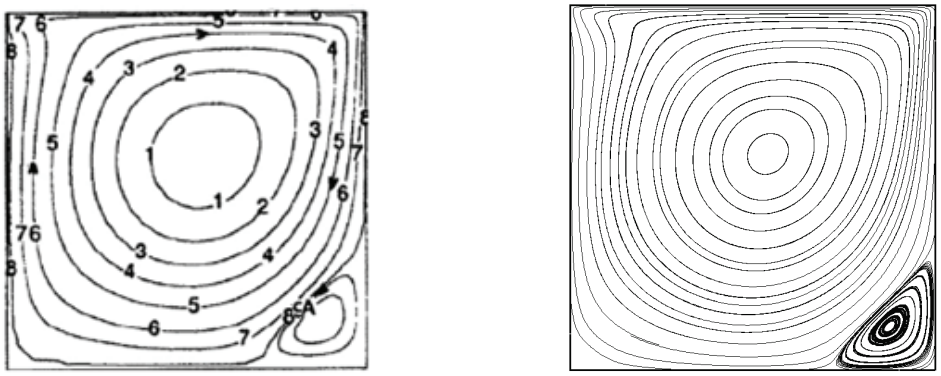

Fig. 2. Comparison of the streamlines between (a) the present study and (b) Moallemi and Jang [6] at Re = 500, Ri = 0.4 and Pr = 1

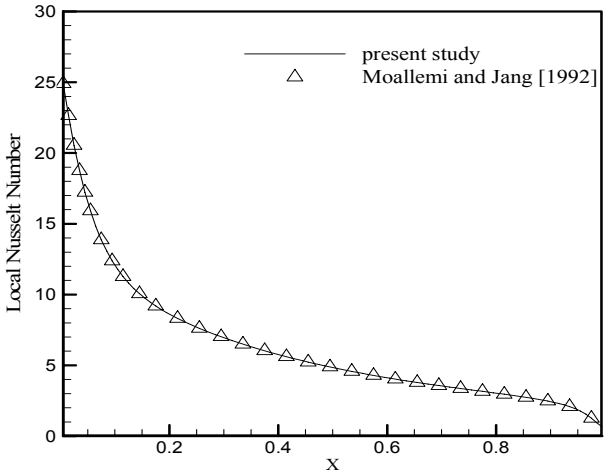

Fig. 3. Comparison of the local Nusselt number variation along the cavity lid between the present results and Moallemi and Jang [6] at Re=500, Ri=0.4, and Pr=1

4. RESULTS AND DISCUSSION

In the present study, the effect of Richardson number and inclination angle of cavity over flow field and heat transfer rate is considered. First, the impact of varying the Richardson number (Ri) on the flow field and temperature contours for various inclination angle is illustrated in Figs. 4 and 5. The Richardson number provides a measurement for the importance of the thermal natural convection forces relative to the mechanically induced lid-driven forced convection effect. It should be mentioned that when Richardson number is more than unity, the natural convection is dominant. For the case with Ri =1 the natural convection effects are comparable to forced convection effects. For dominating forced convection case with Ri=0.01 (Fig. 4), two recirculation bubbles are observed (counter clockwise), one near the hot surface at the left corner of cavity (at $\theta = 0$) and another at the bottom right corner that is bigger than the first bubble, whereas both of them are below the primary bubble (clockwise) that is the biggest. In this case, forced convection is dominante, whereas the inclination has no significant effect on the flow patterns and isotherms. With the increase in Richardson number from 0.01 to 0.1, the effect of forced convection decreases, whereas at positive angle, two small recirculation bubbles below the primary bubble grow.

For the mixed convection case with Ri=1, the effect of inclination angle has a sensitive effect on streamlines and temperature contours (see 5b and 6b). A small recirculation bubble exists below the primary bubble near the right bottom of the cavity for zero inclination. When the cavity is inclined counter-clockwise (0º to 90º), the buoyancy effect opposes forced convection so that the primary bubble

becomes smaller and the secondary bubble expands. In this way, secondary flow does not permit the fluid near the cold lid to move easily to the hot surface. Thus heat transfer from the hot surface in these cases decreases with respect to the previous case. When inclination increases to clockwise (from 0º to-90º), buoyancy and forced convection are in the same direction, whereas the small recirculation bubble is diminished and the primary bubble covers the whole of the cavity. In these cases, the fluid near the cold surface moves easily toward the hot surface.

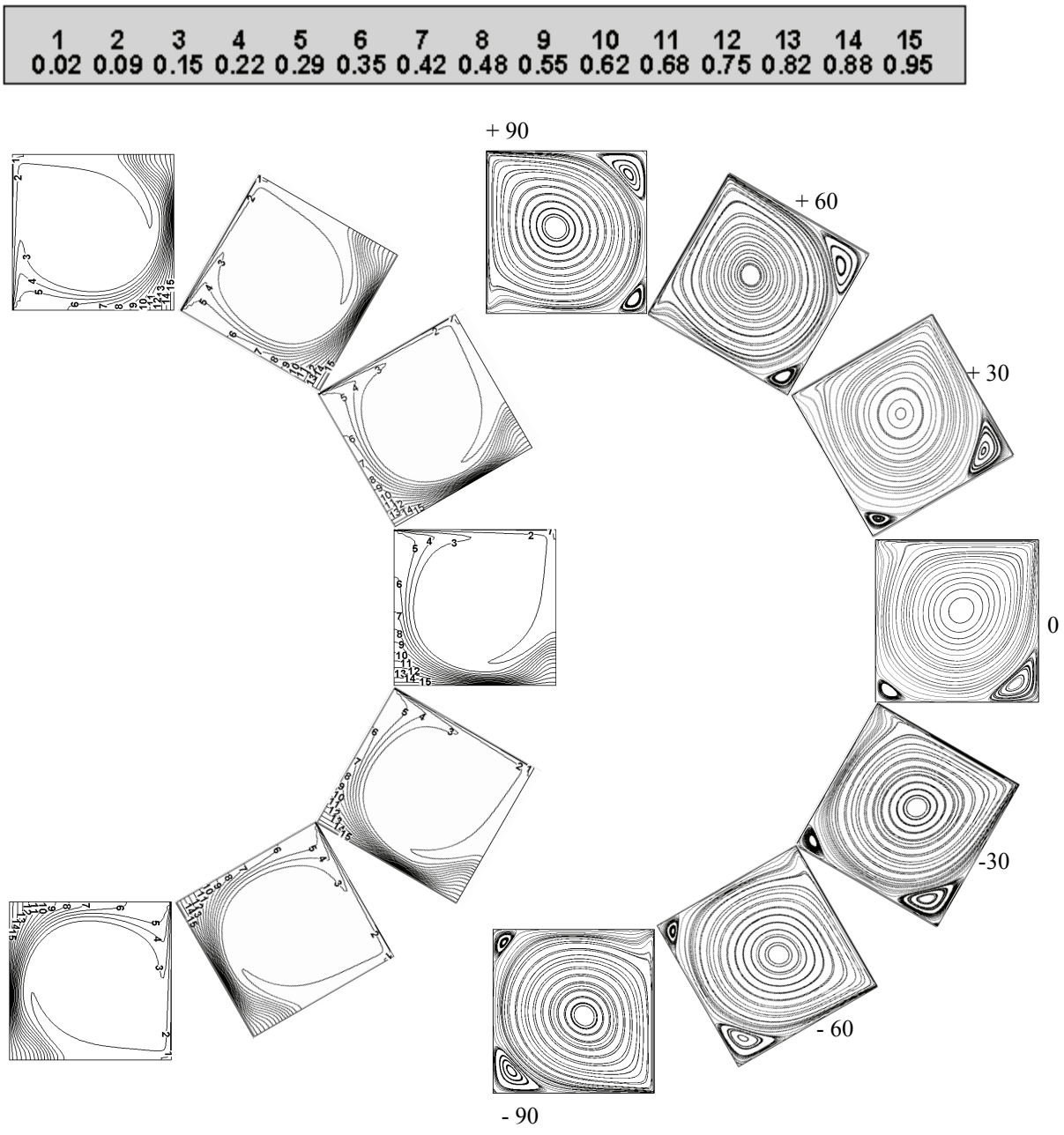

Fig. 4. Streamlines and temperature contour at different inclination angles for Ri=0.01

For the natural convection case with Ri=10, it can be seen that the change of inclination angle has a significant impact on the thermal and hydrodynamic flow field as well as the previous case. When the inclination increases counter-clockwise (form 0 to +90), the small bubble expands due to the buoyancy force, which has more influence on the flow field with respect to the previous case (Ri=1). Also, a thin recirculation bubble can be seen only near the lid because of shear driven flow.

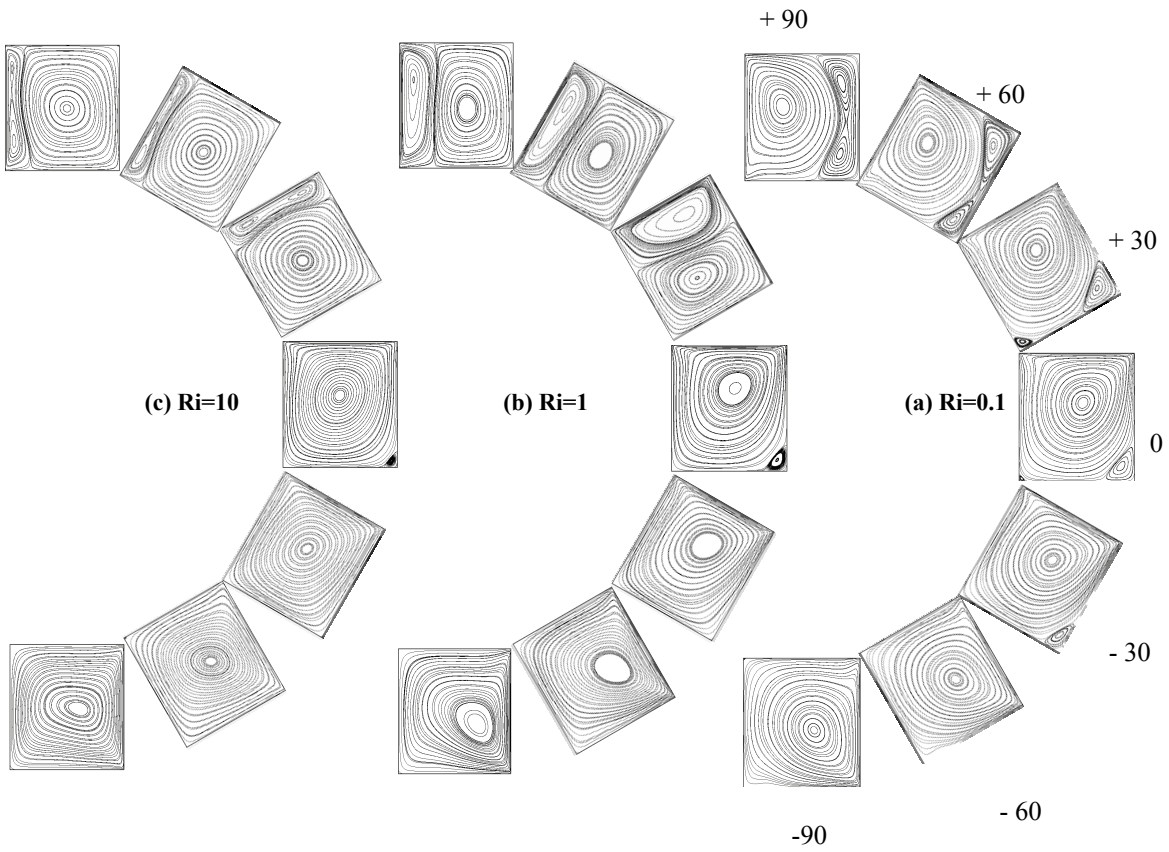

Fig. 5. Streamlines o for various Richardson number at different inclination angles

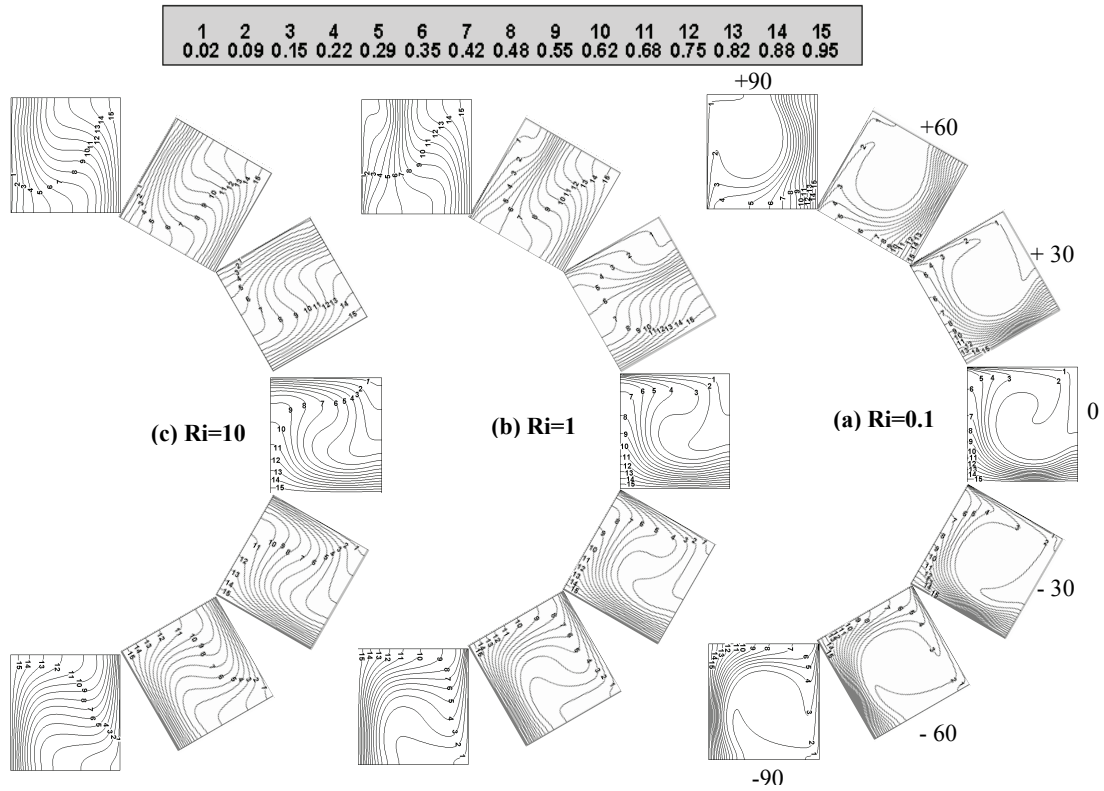

Fig. 6. Temperature contours for various Richardson number at different inclination angle

The variation of local Nusselt number along the hot surface at different inclination of cavity for three Richardson numbers is depicted in Figs. 7 respectively. Nusselt number is independent of inclination angle for low Richardson number (Fig. 7a). It increases first and then decreases for all inclination angles. This is due to the existence of the two recirculation bubbles at the corners of the hot surface.

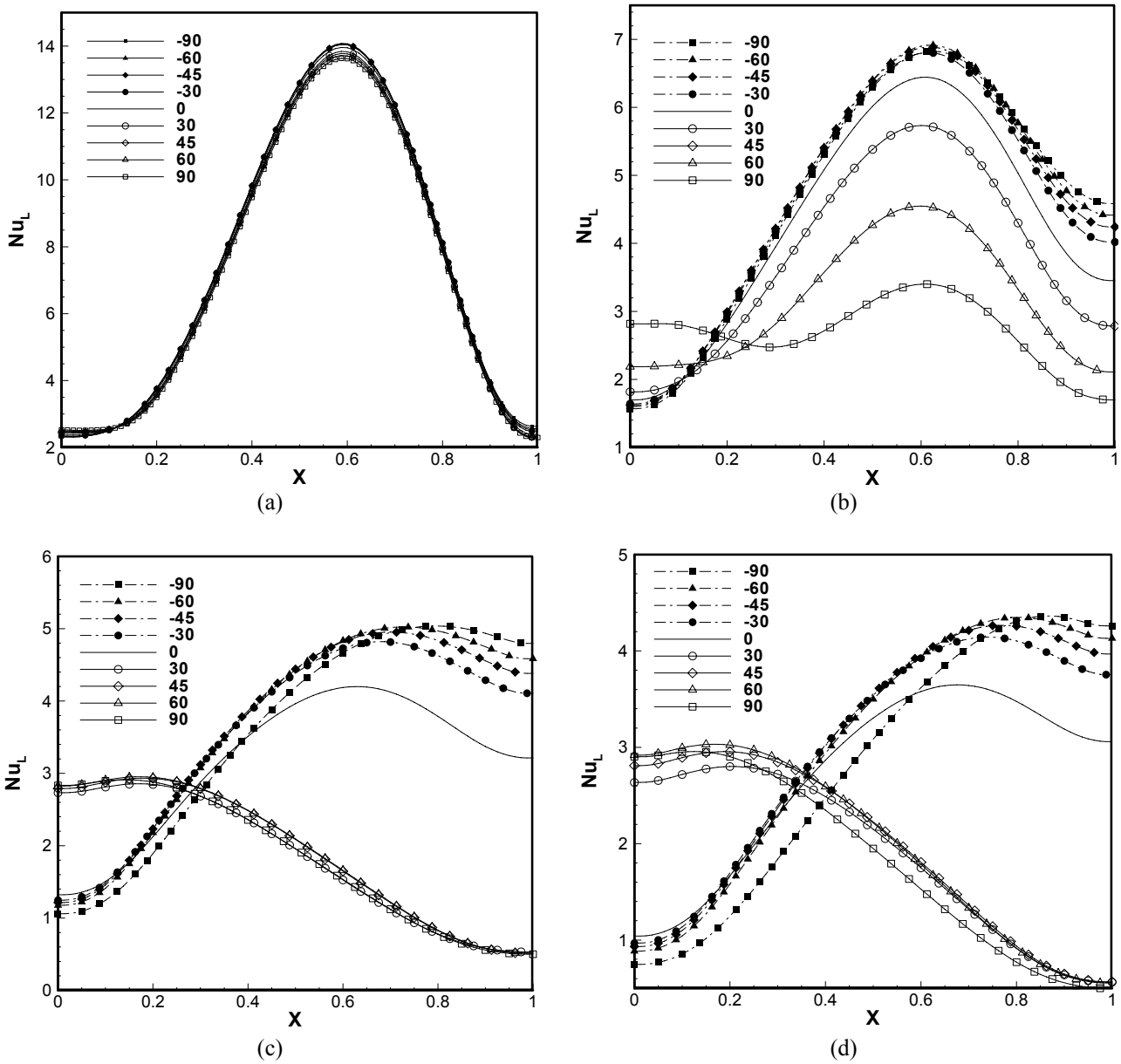

Fig. 7. Distribution of local Nusselt along hot surface of cavity at different inclination angle for (a):Ri=0.01, (b): Ri=0.1, (c): Ri=1 and (d): Ri=10

As mentioned before, by increasing the Richardson number from 0.01 to 0.1, the effect of forced convection decreases, whereas there are two recirculation bubbles (bigger than previous case) at positive inclination angles. It has a negative effect on the heat transfer (see Fig. 7b). By increasing the Richardson number from 0.1 to 1, both forced and natural convections affect the flow field and heat transfer over the surfaces of the cavity. At negative inclination angles, there is only one main vortex core so the Nusselt number is high. On the other hand, there are two vortex cores for positive inclination angles. It has a negative effect on the heat transfer (see Fig. 7c). This phenomenon can be observed at high Richardson number with some discrepancies (Fig. 7d).

The variation of average Nusselt number along the hot surface in various cavity angles from -90º to 90º for different Richardson numbers is plotted in Fig. 8. It is observed that the averaged Nusselt number is independent of inclination angle of cavity for Ri of 0.01. The average Nusselt profile for Ri=0.1 is between profiles for Ri=0.01 and Ri=1 (or Ri=10).

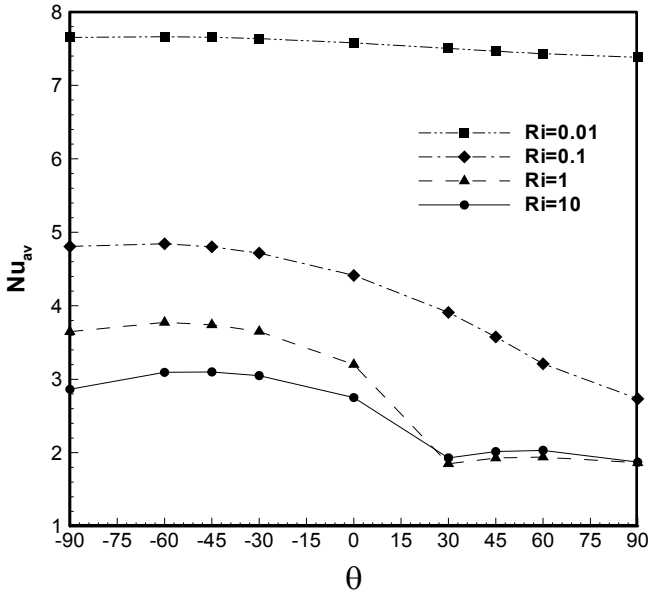

Fig. 8. Variation of average Nusselt versus different inclination angles for various Richardson number

The trend of averaged Nusselt number variation for Ri=1 and Ri=10 is the same. In the negative angle, the buoyancy force and forced convection are in the same direction so heat transfer increases. In the positive angle, as mentioned above, natural convection opposes forced convection and therefore two separate recirculation region forms: one of them is related to natural convection near the hot surface and another is related to movement of the cold lid. In this way, the cold fluid near the lid cannot move downward near the hot surface. Thus, it can be mentioned that the existence of a recirculation bubble near the cold lid causes a decrease in heat transfer from the hot surface significantly. When this recirculation bubble expands (depends on Richardson number and angle of cavity), heat transfer from the hot surface has a greater decrease. This is the reason for turning point in the average Nusselt number profile in 30^{o}.

Maximum heat transfer occurs at an inclination of -60^{o} for all Richardson numbers, particularly for Richardson of 1. This inclination seems to be the optimum position of the cavity where forced and natural convections work together to release the maximum heat transfer rate. At inclination angles less than -60^{o}, forced convection has a greater influence with respect to the natural convection, and vice versa for inclination angles more than -60^{o}.

5. CONCLUSION

Laminar mixed convection for three Richardson numbers that present forced convection dominating, mixed convection and natural convection dominating are investigated using lattice Boltzmann method for various inclination angles of lid-driven cavity. Predicted results show that Nusselt number has no sensitive change with inclination when forced convection dominated (Ri=0.01). For mixed and natural convection dominating (Ri =1 and Ri =10), the overall heat transfer decreases mildly for positive inclination angles where natural and forced convections are opposite each other, while it increases for negative inclination angles where the natural and forced convections have the same direction. Optimum inclination angle with maximum heat transfer is equal to -60^{o}.

NOMENCLATURE

c_k	discrete lattice velocity in direction (k)
c_s	speed of sound in Lattice scale
F_k	external force in direction of lattice velocity
f_k^{eq}	equilibrium distribution
g_y	acceleration due to gravity, (ms^{-2})
H	Height of enclosure (m)
k	thermal conductivity $(W/m.K)$
Nu_{av}	averaged Nusselt number
Nu_L	local Nusselt number along surfaces
Pr	Prandtl number (ν/α)
Ra	Rayleigh number $(g\beta\Delta TH^3/\alpha\nu)$
Ri	Richardson number $(\frac{Gr}{\mathrm{Re}^2})$
Kn	Knudsen number
T_h	hot temperature (K)
T_c	cold temperature (K)
u	velocity (m/s)
w_k	weighting factor

Greek symbols

β	thermal expansion coefficient $(1/K)$
μ	molecular viscosity $(kg/m.s)$
ρ	density (kg/m^3)
τ	lattice relaxation time
Δt	lattice time step

REFERENCES

1. Wang, C. C. & Chen, C. K. (2002). Forced convection in a wavy-wall channel. *Int. J. Heat Mass Tran*., Vol. 45, pp. 2587–2595, [doi:10.1016/S0017-9310(01)00335-0].
2. Al-Amiri, A., Khanafer, K., Bull, J. & Pop, I. (2006). Effect of sinusoidal wavy bottom surface on mixed convection heat transfer in a lid-driven cavity. *Int. J. of Heat and Mass Tran.*, 50: 1771–1780, 2007. [doi:10.1016/j.ijheatmasstransfer.2006.10.008].
3. Al-Amiria, A. M., Khanafer, K. M. & Pop, I. (2007). Numerical simulation of combined thermal and mass transport in a square lid-driven cavity. *Int. J. of Thermal Sciences*, Vol. 46, No. 7, pp. 662-671, [doi:10.1016/j. ijthermalsci.2006.10.003].
4. Molki, M. (1996). Oscillatory heat transfer coefficients in transient natural convection in square cavities. *Iranian J. of Science and Technology, Transaction B, Engineering*, Vol. 20, No. B3, pp. 351-359.
5. Kandasamyk, M., Hashim, I., Khamis, A. B. & Muhaimin, I. (2007). Combined heat and mass transfer in MHD free convection from a wide with ohmic heating and viscous dissipation in the oresence of suction or injection**.** *Iranian Journal of Science & Technology, Transaction A*, Vol. 31, No. A2, pp. 151-162.

6. Moallemi, M. K. & Jang, K. S. (1992). Prandtl number effects on laminar mixed convection heat transfer in a lid-driven cavity. *Int. J. Heat Mass Tran.*, Vol. 35, pp. 1881–1892, [doi:10.1016/0017-9310(92)90191-T]
7. Prasad, A. K. & Koseff, J. R. (1996). Combined forced and natural convection heat transfer in a deep lid-driven cavity flow. *Int. J. Heat Fluid Flow*, Vol. 17, pp. 460–467, [doi:10.1016/0142-727X(96)00054-9].
8. Leong, J. C., Brown, N. M., Lai, F. C. (2005). Mixed convection from an open cavity in a horizontal channel. *Int. Communications in Heat and Mass Transfer*, Vol. 32, pp. 583-592, [doi:10.1016/j.icheatmasstransfer. 2004.10.018].
9. Singh, S. & Sharif, M. A. R. (2004). Numerical study of mixed-convective cooling of a rectangular cavity with differentially heated side walls. *Energy Conversion Engineering Conference*, 2002. IECEC apos; 02. 2002, 37th Intersociety 29-31, pp.765-770.
10. Basak, T., Roy, S., Sharma, P. K. & Pop, I. (2009). Analysis of mixed convection flows within a square cavity with uniform and non-uniform heating of bottom wall. *International Journal of ThermalSciences*, Vol. 52, No. 9-10, pp. 2224-2242, [doi:10.1016/j.ijthermalsci.2008.08.003].
11. Qian, Y. H., d'Humieres, D. & Lallemand, P. (1992). Lattice BGK models for Navier–Stokes equation, Europhys. Lett., Vol. 17 (6), pp. 479–484, 1992, [doi:10.1209/0295-5075/17/6/001].
12. Chen, S. & Doolen, G. D. (1998). Lattice Boltzmann method for fluid flows. *Annu. Rev. Fluid Mech*, Vol. 30, pp. 329–364, [doi:10.1146/annurev.fluid.30.1.329].
13. Yu, D., Mei, R., Luo, L. S., Shyy, W. (2003). Viscous flow computations with the method of lattice Boltzmann equation. *Progr. Aerospace Sci*., Vol. 39, pp. 329–367, [doi: 10.1016/S0376-0421(03)00003-4].
14. Succi, S. (2001). The lattice boltzmann equation for fluid dynamics and beyond. Clarendon Press, Oxford.
15. Fattahi, E., Farhadi, M., Sedighi, K., Nemati, H., Pirouz, M. M. (in press). Effect of Gap-width ratio on natural convection heat transfer in horizontal annulus using LBM. *Heat Trans Res*.
16. Fattahi, E., Farhadi, M., Sedighi, K., Pirouz, M. M. & Nemati, H. (in press). Natural convection and entropy generation in Γ-Shaped enclosure using Lattice Boltzmann method. *Heat Trans Res*.
17. Zhou, Y., Zhang, R., Staroselsky, I., Chen, H. (2004). Numerical simulation of laminar and turbulent buoyancy-driven flows using a lattice Boltzmann based algorithm, Int. J. Heat Mass Transfer, Vol. 47, pp. 4869–4879, [doi:10.1016/j.ijheatmasstransfer.2004.05.020]
18. Dixit, H. N. & Babu, V. (2006). Simulations of high Rayleigh number natural convection in a square cavity using the lattice Boltzmann method. *Int. J. Heat Mass Transfer*, Vol. 49: pp.727–739, 2006. [doi:10.1016/j. ijheatmasstransfer.2005.07.046].
19. Kao, P. H. & Yang, R. J. (2007) Simulating oscillatory flows in Rayleigh–Benard convection using the lattice Boltzmann method, Int. J. Heat Mass Transfer, Vol. 50, pp. 3315–3328, [doi:10.1016/j.ijheatmasstransfer. 2007.01.035].
20. Peng, Y., Shu, C. & Chew, Y. T. (2003). Simplified thermal lattice Boltzmann model for incompressible thermal flows, Phys. Rev. E, Vol. 68, 2003. [doi:10.1103/PhysRevE.68.026701].
21. Barrios, G., Rechtman, R., Rojas, J., Tovar, R. (2005). The lattice Boltzmann equation for natural convection in a two-dimensional cavity with a partially heated wall. *J. Fluid Mech.*, Vol. 522, pp. 91–100, 2005. [doi: 10.1017/S0022112004001983]
22. Delavar, M. A., Farhadi, M. & Sedighi, K. (2009). Effect of the heater location on heat transfer and entropy generation in the cavity using the lattice boltzmann method. *Heat Transfer Research*, Vol. 40, No. 6, pp. 521-536, [doi**:** 10.1615/HeatTransRes.v40.i6].
23. Kao, P. H., Chen, Y. H., Yang, R. J. (2008). Simulations of the macroscopic and mesoscopic natural convection flows within rectangular cavities. *International Journal of Heat and Mass Transfer*, Vol. 51, pp. 3776–3793.
24. [doi:10.1016/j.ijheatmasstransfer.2008.01.003].